

# Notes

## Initial Stage of iPP $\beta$ to $\alpha$ Growth Transition Induced by Stepwise Crystallization

Huihui Li,<sup>†</sup> Xiaoli Sun,<sup>†</sup> Shouke Yan,<sup>\*,†</sup> and Jerold M. Schultz<sup>‡</sup>

State Key Laboratory of Polymer Physics and Chemistry, Institute of Chemistry, Chinese Academy of Sciences, Beijing 100080, P. R. China, Department of Chemical Engineering, University of Delaware, Newark, Delaware 19716

Received December 7, 2007

Revised Manuscript Received April 16, 2008

### Introduction

It is possible to controllably create duplex  $\beta$  and  $\alpha$  isotactic polypropylene (iPP) materials.<sup>1–4</sup> The procedure is based on the temperature dependence of crystal growth rates in  $\alpha$ - and  $\beta$ -iPP. Varga et al.<sup>1,5</sup> have found that the linear growth rate of the  $\beta$  form from the melt is greater than that of the  $\alpha$  form between 100 and 140 °C. Outside this temperature range, the growth rate of  $\alpha$ -iPP is higher than that of  $\beta$ -iPP, and therefore the kinetic condition for the thermodynamically preferred  $\beta$  to  $\alpha$  phase transition is fulfilled. The  $\beta$  to  $\alpha$  growth transition induced by stepwise increment of crystallization temperature is found to be independent of the supermolecular structure of samples studied and happens during spherulitic,<sup>1,2,5</sup> hedritic,<sup>5</sup> and cylindritic<sup>3,6</sup> crystallization. This suggests that the growth transition takes place on the growing  $\beta$ -crystal surface and has been explained in terms of  $\alpha$ -phase nucleation on the growing  $\beta$ -crystal surface.<sup>2</sup>

One procedure for producing duplex  $\alpha$ - $\beta$ -iPP materials is to embed oriented  $\alpha$ -iPP fibers into an iPP melt and then lower the temperature to foster  $\beta$ -iPP growth (140 °C >  $T$  > 100 °C) from the surface of the fibers. The temperature is then raised above 140 °C, where growth continues via the faster growing  $\alpha$  form. As a result, one observes both the inmost  $\beta$  transcrystalline layer grown on the fiber and a second layer of the  $\alpha$  form resulting from the  $\beta$  to  $\alpha$  growth transition.

While most of this process is already well understood for melt-grown single crystals, it is still not known how the  $\alpha$  crystals are initiated at or near the  $\beta$ -form growth front from melt. It is this question that is addressed in the present note.

### Experimental Section

After fiber introduction to the melt at ca. 175 °C, samples are quickly moved to a hotplate set at 134 °C and held there for 0.5 h, to induce isothermal crystallization into the  $\beta$ -form. The samples are then quickly transferred to another hotplate set at 150 °C and held there for 4 h, to induce isothermal crystallization into the  $\alpha$

form, producing a  $\beta$  to  $\alpha$  growth transition. Finally, the material is quenched to room temperature. Details about the polymer used and the procedures outlined above can be found in refs 7 and 8.

Hot-stage optical microscopy and scanning electron microscopy (SEM) were used to observe the morphology of the material. Prior to SEM observation at 15 kV, specimens were etched and gold-coated. Again, details are given in earlier publications.<sup>7,8</sup>

### Results

Figure 1 shows an optical micrograph of material prepared as described above. One can see the fiber-induced transcrystallization layers and spherulites crystallized away from the fiber. Within each spherulite there are two distinct boundaries, indicated by arrows, showing that the crystal growth occurred in three stages, corresponding to the lower and higher isothermal steps and the subsequent cooling process. The iPP crystals in each region of the spherulites are all in the  $\alpha$ -form, while the cylindritic structure surrounding the iPP fiber is composed of the  $\beta$ -cylindrite (directly in contact with the iPP fiber) formed at 134 °C, the  $\alpha$ -iPP layers next to the  $\beta$ -cylindrite, produced isothermally at 150 °C, and finally the thin outer  $\alpha$ -iPP shell formed during the cooling process.

It is instructive to compare the dimensions of simultaneously formed layers in the spherulites and the cylindritic structures. During the lower crystallization temperature stage, the width of the  $\alpha$ -iPP layer grown in the spherulites, ca. 750  $\mu$ m, is much shorter than that induced on the  $\beta$ -iPP cylindrites, approximately 1100  $\mu$ m, consistent with the faster linear growth rate of  $\beta$ -iPP crystals than their  $\alpha$ -counterparts. On the other hand, during the second isothermal crystallization stage at 150 °C, the thickness of the  $\alpha$ -iPP layer in the spherulites ( $\sim$ 300  $\mu$ m) is much longer than that of the isothermal  $\alpha$ -iPP layer of the cylindrite ( $\sim$ 200  $\mu$ m). This can be more precisely determined after separate melting of the  $\beta$ -cylindrite (see Supporting Information) and indicates that time is required for  $\alpha$ -form crystals to nucleate on or near the  $\beta$ -form crystals.

A higher magnification SEM view of the  $\beta$ – $\alpha$  transition

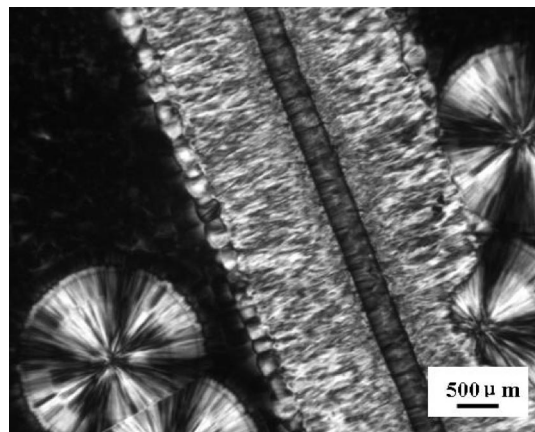


**Figure 1.** Polarized optical micrograph, showing cylindrite growth about inserted fiber and spherulites growing separately in the melt.

\* To whom all correspondence should be addressed. E-mail: skyan@iccas.ac.cn. Telephone: +86-10-82618476. Fax: +86-10-82618476

<sup>†</sup> State Key Laboratory of Polymer Physics and Chemistry, Institute of Chemistry, Chinese Academy of Sciences.

<sup>‡</sup> Department of Chemical Engineering, University of Delaware.



**Figure 2.** Relatively low magnification SEM image showing fan-shaped growth of  $\alpha$ -lamellae from the  $\beta$  growth front.

region is shown in Figure 2. Here  $\alpha$  crystallization has begun near the growth front of  $\beta$  lamellae, seen flat-on at the left. The  $\alpha$ -lamellae are seen edge-on and exhibit the usual cross-hatched pattern inherent to  $\alpha$ -iPP crystallization from the melt.<sup>9–14</sup> The  $\alpha$  crystallization proceeds in a fan-shaped manner, as the  $\alpha$  front of most favorably oriented lamellae overtakes and engulfs the  $\beta$  front. Ultimately the transverse population of  $\alpha$ -lamellae (arrows) dies out.

Details of the  $\beta$  to  $\alpha$  growth transition at the interface are presented in the next series of SEM micrographs. Figure 3a shows  $\alpha$ -iPP lamellae (seen edge-on) growing near the flat-on  $\beta$ -iPP lamellae growth front. A profusion of  $\alpha$ -iPP lamellae form a cross-hatched pattern across the face of the flat-on  $\beta$ -iPP lamellae. Further, some  $\alpha$ -iPP lamellae appear to grow from the between  $\beta$ -iPP lamellae. It is to be noted that the orientation of the  $\alpha$ -lamellae is consistent over the surface of the  $\beta$ -lamella, indicating a role of the  $\beta$  crystals in directing the crystallization of  $\alpha$  crystals.

In Figure 3b, an early growth stage of the  $\alpha$  crystals on the face of the flat-on  $\beta$ -iPP lamellae is seen. Their different lengths may indicate that these  $\alpha$ -iPP lamellae have not initiated simultaneously. In general, the growth direction of the nascent  $\alpha$ -iPP lamellae is the same as that of the  $\beta$  lamellae. Some  $\alpha$ -iPP lamellae at a very early growth stage are noted by the white circles. All three of the numbered  $\alpha$ -lamellae grow initially with a small height above the  $\beta$ -lamella, but the longest of these (crystal 3) appears to have gradually grown farther above the  $\beta$ -lamella. Since the  $\alpha$ -lamellae are seen edge-on, this result demonstrates that growth occurs both in the mean growth direction and transverse to it (as expected). One senses in Figure 3a that the cross-hatched structure of  $\alpha$  lamellae exist not only on the exposed  $\beta$  surfaces but also between the  $\beta$ -lamellae. This sense is reinforced by observation of a large number of SEM micrographs. This behavior indicates that nucleation of  $\alpha$  crystals on the  $\beta$  substrate takes time, allowing the  $\beta$ -lamellae to grow forward over the nascent  $\alpha$ -crystals before the  $\alpha$ -crystals can catch up with the  $\beta$  crystallization front. This finding agrees with the optical microscope finding that the second stage ( $\alpha$ -phase) growth layer of the cylindrites is shorter than the simultaneously forming second layer of the spherulites.

## Discussion

A brief discussion focuses on the relationship between the  $\alpha$ -crystals and the  $\beta$  substrate lamella. The only extant study of

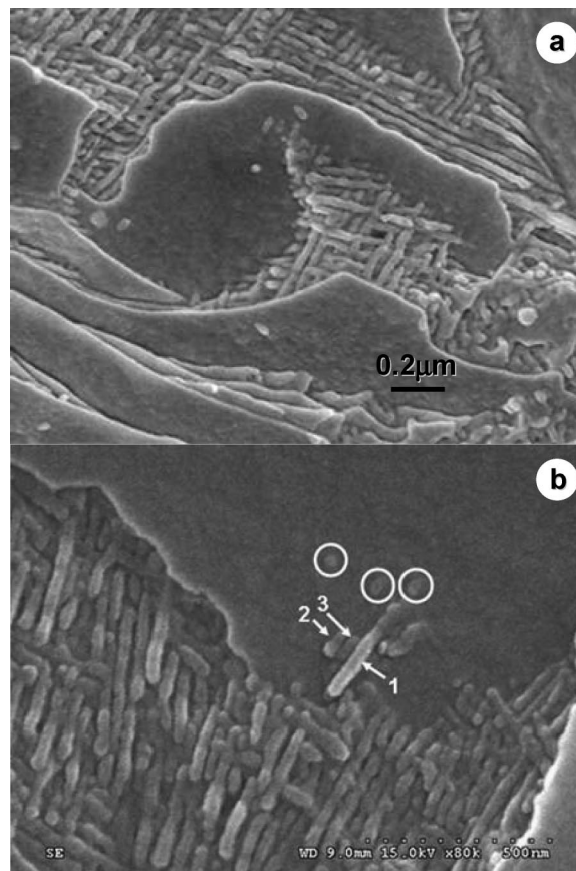


**Figure 3.** SEM images of cross-hatched structures of  $\alpha$  iPP lamellae formed on the surface of  $\beta$ -lamellae: (a) typical area; (b) area showing early stages of  $\alpha$  crystal formation.

$\alpha$  crystals initiated from  $\beta$  crystals deals with  $\alpha$  crystals formed through growth transition induced by temperature jumps and partial melting in single crystals of the  $\beta$  phase.<sup>15,16</sup> In that case, Lotz and co-workers report that  $\alpha$  crystals grow epitaxially from the (110) lateral growth faces of the  $\beta$  single crystals, with the chains in the two forms parallel and the lateral (010) face of the  $\alpha$ -form parallel to the (110) of the  $\beta$  crystal. In the present case, the consistency of the directions of the parallel  $\alpha$  crystals indicates that they are somehow directed by the underlying  $\beta$ -lamella. Unfortunately, the crystallographic relationship between the  $\beta$  substrate and the  $\alpha$ -lamellae cannot be known from the present results. Therefore, we can only make a conjecture about the underlying physics. According to the crystallographic registry determined in the partially molten  $\beta$ -iPP single crystal,<sup>15,16</sup> the situation would be as depicted in Figure 4a; i.e., the  $\alpha$ -phase mother lamellae lie in the same plane as the  $\beta$  lamellae and would grow transverse to the growth direction of the  $\beta$  lamellae, while the daughter  $\alpha$  lamellae would sit at  $80^\circ$  to the mother, growing steeply out of the plane of view. This will lead to the situation that the initial mother lamellae and all of the even number generations of daughters would then be viewed flat-on and the odd-numbered daughter lamellae edge-on. This cannot be the case, since in that way the mother and the daughter lamellae should be seen perpendicular to each other, as depicted in Figure 4b, rather than  $80^\circ$  apart, as demanded by homoepitaxy (depicted in Figure 4c), and which is actually observed in present case. Moreover, it is highly unlikely that the edge-on and flat-on lamellae exhibit the same width (normal to the lamellar growth direction), as is commonly seen (in other work) in mother/daughter sets viewed edge-on. Therefore, it appears that the orientation relationship between  $\alpha$  and  $\beta$  crystals

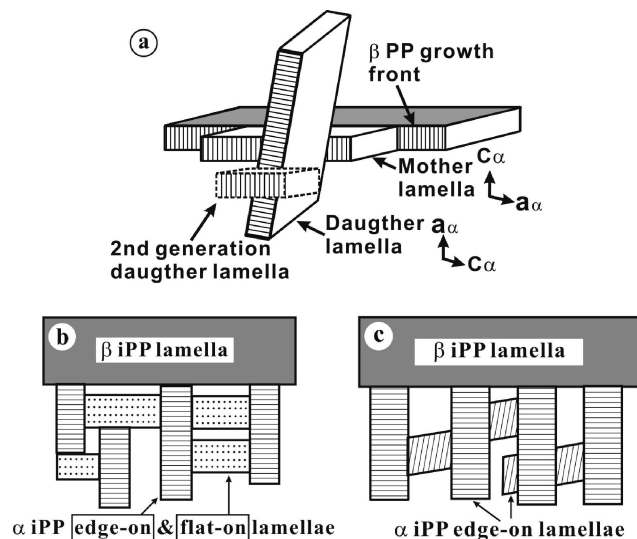


**Figure 4.** (a) Three-dimensional sketch and (b) its corresponding two-dimensional projection along the  $c$ -axis of  $\beta$ -iPP crystal illustrating the  $\beta$  to  $\alpha$  growth transition of iPP according to the reported crystallographic registry. (c) Sketch describing the observed morphology in the present work.

here is somewhat different from that reported by Lotz and co-workers for partially melted and recrystallized single crystals of the beta form. There is not sufficient information to speculate further on either the orientations of the lamellae or on their genesis. These questions are intriguing and should be examined in future work.

**Acknowledgment.** Financial support of the Outstanding Youth Fund and the National Natural Science Foundation of China (No.

50521302, 20574079, 20634050 and 20604031) are gratefully acknowledged.

**Supporting Information Available:** Figure showing the optical micrographs before and after selective melting of a sample prepared by introducing the iPP fiber into the iPP melt at 174 °C and then crystallized isothermally at 134 and 150 °C, respectively. This material is available free of charge via the Internet at <http://pubs.acs.org>.

## References and Notes

- (1) Varga, J. *J. Mater. Sci.* **1992**, 27, 2557.
- (2) Varga, J.; Fujiwara, Y.; Ille, A. *Period. Polytech. Chem. Eng.* **1990**, 34, 255.
- (3) Varga, J. *Poly(propylene): Structure, Blends and Composites*; Karger-Kocsis, J., Ed.; Chapman & Hall: London, 1995; Vol. 1, 56.
- (4) Varga, J. *J. Therm. Anal.* **1986**, 31, 165.
- (5) Varga, J. *J. Macromol. Sci., Phys.* **2002**, B41, 1121.
- (6) Varga, J.; Karger-Kocsis, J. *J. Polym. Sci., Part B: Polym. Phys.* **1996**, 34, 657.
- (7) Li, H.; Jiang, S.; Wang, J.; Wang, D. J.; Yan, S. K. *Macromolecules* **2003**, 36, 2802.
- (8) Li, H.; Zhang, X.; Kuang, X.; Wang, D. J.; Li, L.; Yan, S. K. *Macromolecules* **2004**, 37, 2847.
- (9) Khoury, F. J. *Res. Natl. Bur. Stand., Sect. A.* **1966**, 70A, 29.
- (10) Padden, F. J., Jr.; Keith, H. D. *J. Appl. Phys.* **1966**, 37, 4013.
- (11) Binsbergen, F. L.; De Lange, B. G. M. *Polymer* **1968**, 9, 23–40.
- (12) Lotz, B.; Wittmann, J. C. *J. Polym. Sci., Part B: Polym. Phys.* **1986**, 24, 1541.
- (13) Lotz, B.; Wittmann, J. C.; Lovinger, A. J. *Polymer* **1996**, 37, 4979.
- (14) Olley, R. H.; Bassett, D. C. *Polymer* **1989**, 30, 399.
- (15) Lotz, B. *Polymer* **1998**, 39, 4561.
- (16) Lotz, B. *J. Macromol. Sci. Phys.* **2002**, B41, 685.

MA702725G